

miR-372-3p is a potential diagnostic factor for diabetic nephropathy and modulates high glucose-induced glomerular endothelial cell dysfunction via targeting fibroblast growth factor-16

Zhiyun Meng, Fangyuan Li, Bin Wang

Department of Nephrology, Weifang City Traditional Chinese Medical Hospital, Weifang, Shandong Province, China

Submitted: 3 June 2019; **Accepted:** 6 September 2019

Online publication: 11 November 2019

Arch Med Sci 2023; 19 (3): 703–716

DOI: <https://doi.org/10.5114/aoms.2019.89659>

Copyright © 2019 Termedia & Banach

Corresponding author:

Dr. Bin Wang
Department
of Nephrology
Weifang City
Traditional Chinese
Medical Hospital
1055 Weizhou Road
Weifang 261041
Shandong Province
China
Phone/fax:
+86 0536-8060705
E-mail:
wang_binwf@aliyun.com

Abstract

Introduction: Previous studies have reported that microRNAs are implicated in the pathogenesis of diabetic nephropathy (DN). In this study, the underlying molecular mechanisms and diagnostic significance of miR-372-3p were investigated in the process of DN.

Material and methods: Cell proliferation and apoptosis were measured using MTT and Annexin V-FITC double staining, respectively. RT-qPCR and western blotting were used to measure the expression levels of mRNA and protein. The diagnostic power of miR-372-3p in plasma for DN was evaluated using the receiver operating characteristics (ROC) curves and the area under the ROC curves (AUC).

Results: miR microarray analysis revealed that 126 miRs were significantly differentially expressed in response to high glucose stimulation. Among these miRs, high glucose stimulated miR-372-3p expression at the highest level. *In vitro* experimental measurements showed that knockdown of miR-372-3p showed the ability to reverse high glucose-induced glomerular endothelial cell apoptosis and impairment of eNOS/NO bioactivity. Mechanistic analysis revealed that fibroblast growth factor-16 (FGF-16) as a direct of miR-372-3p protected against high glucose-induced glomerular endothelial cell dysfunction. ROC analysis revealed that the diagnostic value of miR-372-3p, miR-15a or miR-372-3p combined with miR-15a in type 2 diabetes mellitus patients (AUC = 0.841, $p < 0.001$; AUC = 0.822, $p < 0.001$ or AUC = 0.922, $p < 0.001$) with DN was better than in type 1 diabetes mellitus patients (AUC = 0.805, $p < 0.001$; AUC = 0.722, $p < 0.001$ or AUC = 0.865, $p < 0.001$) with DN.

Conclusions: miR-372-3p might be a valuable therapeutic target and diagnostic marker for patients with DN.

Key words: diabetic nephropathy, glomerular endothelial cells, miR-372-3p, diagnosis.

Introduction

Diabetic nephropathy (DN) is one of the most common complications of patients with type I or type II diabetes mellitus and has been posited to be the second leading cause of end-stage renal disease, and approximately 1/5 of type I and 1/3 of type II diabetic patients are plagued by DN [1, 2]. Microalbuminuria and an increase in urinary albumin excretion

rate (UAER; $\geq 20 \mu\text{g}/\text{min}$) are considered as the early physiological changes in response to renal dysfunction [3]. Although extensive underlying pathogenic mechanisms have been investigated in various renal cells, including podocytes, glomeruli mesangial cells and glomerular endothelial cells [4, 5], the potential molecular targets have not been completely expounded in the pathological process of DN.

microRNAs (miRs) as a new class of non-coding RNAs have been implicated in various physiological and pathological processes via post-transcriptional repression of target gene expression [6]. Interestingly, numerous miRs are already used as therapeutic and diagnostic markers in a variety of diseases, including DN [7, 8]. A systematic review using bioinformatic analysis for evaluating the association between miR expression and DN revealed that five up-regulated miRs, miR-21-5p, miR-29a-3p, miR-126-3p, miR-214-3p, and miR-342-3p, and one down-regulated miR, miR-192-5p, are involved in the pathogenesis of DN [9]. Glomerular endothelial cell-specific miRs, such as miR-146a, 155 and miR-497, are activated in high glucose condition and contribute to glomerular endothelial injury [8, 10]. In addition, serum miR-130b and miR-21 and urinary miR-192, let-7c-5p, miR-29c-5p and miR-15b-5p have been reported as potential diagnostic biomarkers for DN [11–14]. Four differentially expressed miRs, miR-21-3p, miR-378-3p, miR-16-5p and miR-29a-3p, in plasma are closely correlated with the pathological grade of patients with DN [15].

In the present study, we used miR microarray analysis to explore miR expression profiling in high glucose-treated human glomerular endothelial cells, and found that 126 miRs were significantly differentially expressed in glomerular endothelial cells in response to high glucose stimulation. The

expression of the top 6 miRs, miR-372-3p, miR-15a, miR-555, miR-let-7i-5p, miR-621 and miR-646, was observed in high glucose-stimulated glomerular endothelial cells using RT-qPCR, and the results demonstrated that miR-372-3p was noteworthy for glomerular endothelial cell dysfunction. Moreover, we also measured the expression level of miR-372-3p in the serum of patients with DN to evaluate whether miR-372-3p might be a valuable diagnostic factor for DN screening. Furthermore, we discovered that fibroblast growth factor-16 (FGF-16), which belongs to the FGF-9 subfamily and mainly exerts protective effect on heart [16], as a direct target of miR-372-3p was associated with high glucose-induced glomerular endothelial cell dysfunction.

Material and methods

Patients and specimens

Fifty-seven healthy controls (HC), fifty-three type 1 diabetes mellitus (T1DM) and one hundred and eighteen type 2 diabetes mellitus (T2DM) patients with DN were enrolled in the Weifang City Traditional Chinese Medical Hospital from January 2015 to December 2018. Clinical and laboratory characteristics of HC and T1DM or T2DM patients with DN were summarized as shown in Table I. The diagnostic criteria of T1DM and T2DM were adopted as described previously [17]. The inclusion and the exclusion criteria of T1DM or T2DM patients with DN were as follows: inclusion criteria were patients diagnosed with DN combined with T1DM or T2DM and age less than 80 years; exclusion criteria were kidney transplantation, nondiabetic nephropathy, acute cerebrovascular events, acute coronary events and acute infectious diseases, malignant tumor, chronic rheumatic disease, and thyroid function abnormalities. Whole blood (10 ml) was collected from all participants, and plas-

Table I. Clinical and laboratory characteristics of HC and patients with DN

Parameter	HC (n = 57)	T2DM patients with DN (n = 118)	T1DM patients with DN (n = 53)
Age [years]	52.6 \pm 14.7	54.7 \pm 12.1	30.2 \pm 18.9*
Gender (M/F)	31/26	63/55	27/26
BMI [kg/m ²]	23.8 \pm 3.2	28.4 \pm 3.9*	21.5 \pm 3.41
Duration of DN [years]	–	4.6 \pm 1.7	3.8 \pm 1.5
FBG [mmol/l]	4.83 \pm 0.68	7.15 \pm 1.41*	10.63 \pm 1.61*
HbA _{1c} (%)	5.12 \pm 0.45	8.33 \pm 1.66*	9.65 \pm 2.05*
Scr [$\mu\text{mol}/\text{l}$]	52.5 \pm 5.2	78.5 \pm 8.5*	100.4 \pm 9.7*
eGFR [ml/min/1.73 m ²]	129.4 \pm 20.55	70.6 \pm 25.1*	65.3 \pm 26.9*

HC – healthy controls, DN – diabetic nephropathy, T1DM – type 1 diabetes mellitus, T2DM – type 2 diabetes mellitus, M – male, F – female, BMI – body mass index, FBG – fasting blood glucose, HbA_{1c} – glycosylated hemoglobin, Scr – serum creatinine, eGFR – estimated glomerular filtration rate. *P < 0.05 compared with the healthy control group.

ma was separated as described previously [18]. Signed informed consent forms were obtained from all patients. Our study was approved by the Ethics Committee of the Weifang City Traditional Chinese Medical Hospital.

Cell culture

Human glomerular endothelial cells were obtained from ScienCell Research Laboratories (Carlsbad, CA, USA) and cultured in Dulbecco's modified Eagle's medium (DMEM; Gibco; Thermo Fisher Scientific, Inc., Waltham, MA, USA), containing 10% fetal calf serum (Gibco; Thermo Fisher Scientific, Inc.), 10% L-glutamine, 0.5% penicillin/streptomycin, with 5% CO₂ atmosphere at 37°C.

Microarray assays

Microarray analysis was performed using Agilent Human miRNA (8*15K) V14.0 arrays of Ribobio (Guangzhou, China), as described previously [19]. In brief, after the human glomerular endothelial cells' exposure to high glucose (30 mM) or normal glucose (5 mM), miR expression profiling was detected using miR microarray assays ($n = 3$ in each group). The miRNeasy Mini Kit (Qiagen, Inc., Valencia, CA, USA) was used to extract total RNA, according to the manufacturer's protocol. miRs were labeled with Hy3 or Hy5 fluorescence using the miRCURY Array Power Labeling Kit (Exiqon) to obtain the fluorescent probe that can be hybridized with the chip. The labeled probe was hybridized with the miRCURY chip under the standard conditions using the MAUI hybridization system. An Agilent scanner and the Feature Extraction 10.7.1.1 software (Agilent Technologies) were used to obtain the microarray raw data. Microarray results were analyzed using the GeneSpring GX 12.5 software (Agilent Technologies). Differentially expressed miRs were selected out according to $|\text{Log}_2 \text{fold change}| \geq 1$, $p < 0.05$ and a false discovery rate < 0.05 . The hierarchical clustering analysis was performed using MeV software (version 4.2.6).

RNA isolation and RT-qPCR

The miRNeasy Mini Kit (Qiagen, Inc., Valencia, CA, USA) was used to extract total RNA, according to the manufacturer's protocol. The TaqMan RT kit and TaqMan MicroRNA assay (Thermo Fisher Scientific, Inc.) were used to perform RT-qPCR assay of miRs using the Applied Biosystems StepOne-Plus Real-Time PCR System. The reaction was performed via 40 amplification cycles using the following protocol: 95°C for 3 min, 95°C for 45 s, 55°C for 15 s, and 72°C for 50 s. miRs expression levels were calculated using the $2^{-\Delta\Delta C_t}$ method, as previously described [20]. U6 was used as an

internal control. The primers used for PCR were as follows: miR-372-3p: forward, 5'-TTTCACGACGCTGTAAGCTCGCA-3', and reverse, 5'-GTGCA-GGGTCCGAGGT-3'; miR-15a forward, 5'-TAGCAGCACATAATGGTTTGTG-3', and reverse, 5'-GTG-CAGGGTCCGAGGT-3'; U6 forward, 5'-CTCGCTC-GGCAGCACA-3', and reverse, 5'-AACGCTTCAC-GAATTTGCG-3'.

MTT assay

Glomerular endothelial cell proliferation was monitored using a MTT Cell Proliferation/Viability Assay kit (R&D Systems, Inc., Minneapolis, MN, USA) according to the manufacturer's protocol.

Nitric oxide (NO) production

The level of NO in cellular supernatant was detected using the bioactive ELISA assay (Elabscience Biotechnology Co., Ltd., Wuhan, China) with a SpectraMax M5 ELISA plate reader (Molecular Devices, LLC, Sunnyvale, CA, USA), according to the manufacturer's protocol.

Malondialdehyde (MDA)

Glomerular endothelial cells were lysed with extraction buffer and centrifuged (12000×g, 10 min, 4°C) for collecting supernatant. MDA was detected using a commercial kit from the Nanjing Jiancheng Bioengineering Institute (Nanjing, China).

Caspase-3 activity

Glomerular endothelial cells lysates were prepared and incubated with anti-caspase 3 (cat. no: 9662; dilution: 1 : 50; Cell Signaling Technology, USA). Immunocomplexes were incubated with peptide substrate in assay buffer for 2 h at 37°C. Release of p-nitroaniline was measured at 405 nm using an ELISA reader (MD SpectraMax M5, USA) according to the manufacturer's instructions.

Western blotting

Western blotting assay were determined as previously described [21]. eNOS (cat. no: 9586; dilution: 1 : 1,000) and p-eNOS (cat. no: 9571; dilution: 1 : 1,000) primary antibodies were purchased from Cell Signaling Technology. FGF-16 (cat. no: sc-376214; dilution: 1 : 1,000) antibody was purchased from Santa Cruz Biotechnology. Anti-β-actin (cat. no. sc-130065; 1 : 2,000; Santa Cruz Biotechnology) was used as the control antibody.

Cell apoptosis assay

The cell apoptosis assay was determined as previously described [22]. The Annexin V-FITC

apoptosis detection kit was purchased from Invitrogen (Carlsbad, Calif, USA). The samples were analyzed using a flow cytometer (BD Biosciences, Franklin Lakes, NJ, USA).

Cell transfection and plasmid constructs

miR-372-3p mimics (5'-AAAGUGCUGCGACAUUUGAGCGU-3'), inhibitors (5'-ACGCUCAAUGUCG-CAGCACUUU-3') and scramble sequence (5'-CUAUGUGUCUCUGUAUAGUUAGC-3') were synthesized by RiboBio (Guangzhou, China) and transfected with into glomerular endothelial cells using Lipofectamine 2000 (Invitrogen) for 48 h at 37°C according to the manufacturer's protocol. A mammalian expression plasmid designed to specially express the full-length open reading frame of human *FGF-16* without 3'-UTR, which did not contain the conserved complementary sequence binding with miR-372-3p, was purchased from GeneCopoeia, Inc. (Rockville, MD, USA). An empty plasmid served as the negative control. Vector-Con and vector-*FGF-16* were transfected into HCC cells using Lipofectamine 2000 for 48 h at 37°C, according to the manufacturer's protocols.

Luciferase reporter gene assay

The wild-type (WT) or mutant-type (Mut) 3'-UTR of *FGF-16* were inserted into the multiple cloning sites of the luciferase expressing the pMIR-REPORT vector (Ambion; Thermo Fisher Scientific, Inc.). The luciferase activity was measured using the Dual Luciferase Reporter Assay System (Promega, USA) on a Luminoskan Ascent Microplate Luminometer (Thermo Fisher Scientific, Waltham, MA, USA).

Statistical analysis

Data were presented as the mean \pm standard error of the mean. Statistical analysis was performed using SPSS software version 19.0 (IBM Corp., Armonk, NY, USA) and GraphPad Prism version 7.0 (GraphPad Software, Inc., La Jolla, CA, USA). Student's *t*-test was used to analyze two-group differences. Differences between multiple groups were analyzed by one-way analysis of variance, followed by a post-hoc Tukey test. Receiver operating characteristic (ROC) curves and the area under the ROC curve (AUC) were used to assess the potential for using plasma miR-372-3p and miR-15a as diagnostic biomarkers of DN. Binary logistic regression analysis was used to combine the expression level of miR-372-3p and miR-15a as combined diagnostic markers for DN. The maximum value of the Youden index was used as a criterion for selecting the optimum cut-off point. $P < 0.05$ was considered to indicate a statistically significant difference.

Results

miRs expression profiles in high glucose-stimulated glomerular endothelial cells

Specific miRs responsive to high glucose stimulation in glomerular endothelial cells were identified to excavate valuable therapeutic targets for the treatment of DN. miRs microarray assays were used to analyze differentially expressed miRs. A total of one hundred and twenty-six miRs, which were selected out according to $|\text{Log}_2 \text{fold change}| \geq 1$, $p < 0.05$ and false discovery rate < 0.05 , were found to be significantly and differentially expressed between normal glucose and high glucose-treated glomerular endothelial cells (Figure 1 A). To further investigate the function of miRs in pathophysiological conditions of glomerular endothelial cells, we focused on the top six differentially expressed miRs, comprising two up-regulated miRs (miR-15a and miR-372-3p) and four down-regulated miRs (miR-555, miR-let-7i-5p, miR-621 and miR-646). We also validated these miRs' expression levels in high glucose-stimulated glomerular endothelial cells using RT-qPCR assays (Figure 1 B). Finally, miR-372-3p was considered as the most sensitive miR in response to high glucose-stimulated glomerular endothelial cells and selected for further study.

Knockdown of miR-372-3p reverses high glucose-induced glomerular endothelial cell dysfunction

After transfection with miR-Con or miR-372-3p inhibitors into high glucose-treated glomerular endothelial cells, MTT assays were performed to detect the effects of high glucose and miR-372-3p inhibitors on glomerular endothelial cell proliferation. Compared with the normal glucose-treated group, cell viability was significantly repressed in glomerular endothelial cells stimulated by high glucose for 48 h and 72 h, while miR-372-3p loss-of-function markedly reversed high glucose-induced glomerular endothelial cell growth inhibition (Figure 2 A). In addition, transfection with miR-Con into glomerular endothelial cells had no obvious effect on cell viability in high glucose (30 mM)-stimulated cells (Figure 2 A). Previous studies have reported that high glucose can impair production of endothelial nitric oxide synthase (eNOS) and NO, which performs the predominant role in endothelial cell dysfunction by regulating oxidative stress [5, 23]. Reduced phosphorylation of eNOS at Ser1179 has been observed in high glucose-stimulated glomerular endothelial cells and both diabetic mouse and rat [24, 25]. Our results also indicated that high glucose treatment significantly decreased NO production and the protein expression of phosphorylated eNOS at Ser1179, while knockdown of miR-372-3p dramatically ac-

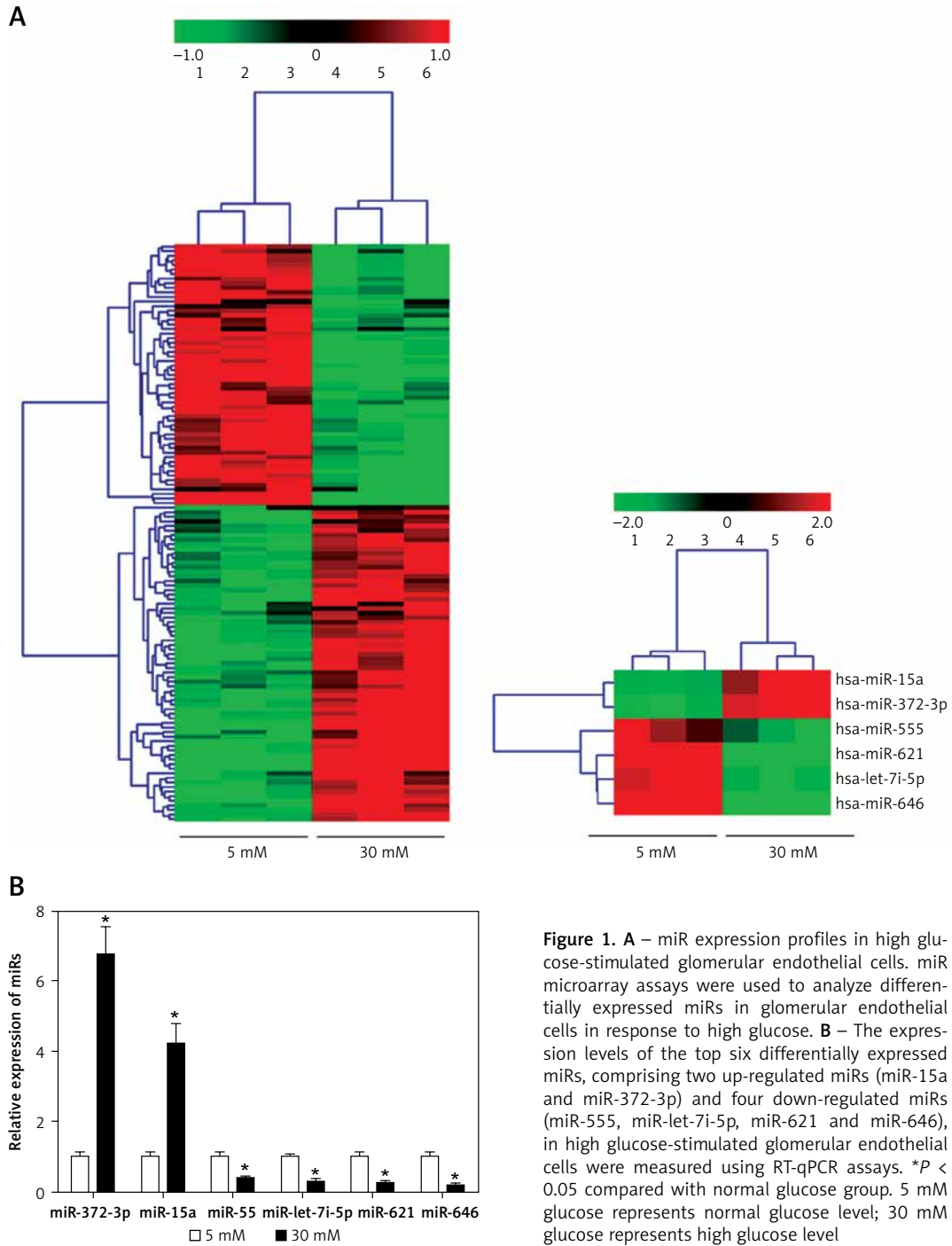


Figure 1. A – miR expression profiles in high glucose-stimulated glomerular endothelial cells. miR microarray assays were used to analyze differentially expressed miRs in glomerular endothelial cells in response to high glucose. **B** – The expression levels of the top six differentially expressed miRs, comprising two up-regulated miRs (miR-15a and miR-372-3p) and four down-regulated miRs (miR-555, miR-let-7i-5p, miR-621 and miR-646), in high glucose-stimulated glomerular endothelial cells were measured using RT-qPCR assays. * $P < 0.05$ compared with normal glucose group. 5 mM glucose represents normal glucose level; 30 mM glucose represents high glucose level

celerated NO production and the protein expression of phosphorylated eNOS at Ser1179 in high glucose-stimulated glomerular endothelial cells (Figures 2 B, 3 C). Next, we analyzed the effects of high glucose and miR-372-3p on MDA production, which is a critical index of lipid peroxidation [26]. High glucose treatment observably triggered an MDA level increase in glomerular endothelial cells. Transfection with miR-372-3p inhibitors significantly lowered the high glucose-induced MDA level (Figure 2 D). Furthermore, miR-372-3p inhibitors

had the ability to prevent high glucose-induced cell apoptosis, reflecting the reduced apoptotic cell proportion and caspase 3 level in glomerular endothelial cells (Figures 2 E, D).

FGF-16 is a direct target of miR-372-3p

The bioinformatics algorithm revealed that a conserved complementary pairing sequence was observed between the 3'-UTR of FGF-16 and miR-372-3p (Figure 3 A). Luciferase activity assay indicated that transfection with miR-372-3p mim-

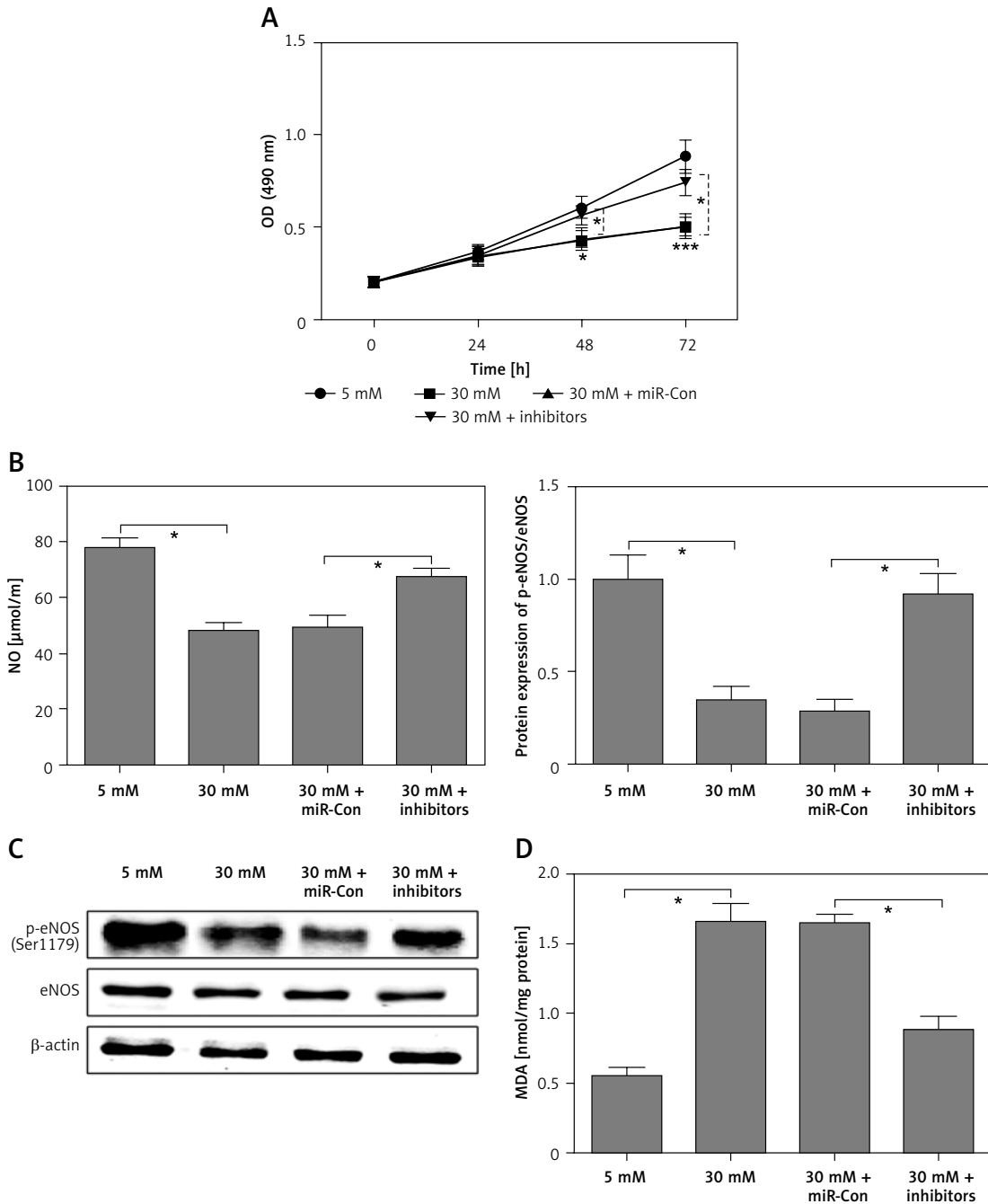


Figure 2. Knockdown of miR-372-3p reverses high glucose-induced glomerular endothelial cell dysfunction. **A** – After transfection with miR-372-3p inhibitors or miR-Con into glomerular endothelial cells in the presence of normal (5 mM) or high glucose (30 mM), cell viability was monitored using MTT assay; **B** – NO production in cellular supernatant was detected using colorimetric assay kit; **C** – eNOS and phosphorylated eNOS were measured using western blotting; **D** – MDA level in supernatant was detected using colorimetric assay kit

ics into glomerular endothelial cells containing the WT 3'-UTR of FGF-16 led to a significant decrease in luciferase activity, suggesting that miR-372-3p could directly bind to the 3'-UTR of FGF-16 (Figure 3 B). Subsequently, the protein expression of FGF-16 was dramatically reduced in glomerular endothelial cells transfected with miR-372-3p mimics compared with these cells transfected with miR-Con (Figure 3 C). These results demonstrated that

miR-372-3p could regulate FGF-16 protein expression via post-transcriptional repression.

Overexpression of FGF-16 alleviates high glucose-induced glomerular endothelial cell dysfunction

To further investigate the roles of FGF-16 in the process of high glucose-induced glomerular en-

miR-372-3p is a potential diagnostic factor for diabetic nephropathy and modulates high glucose-induced glomerular endothelial cell dysfunction via targeting fibroblast growth factor-16

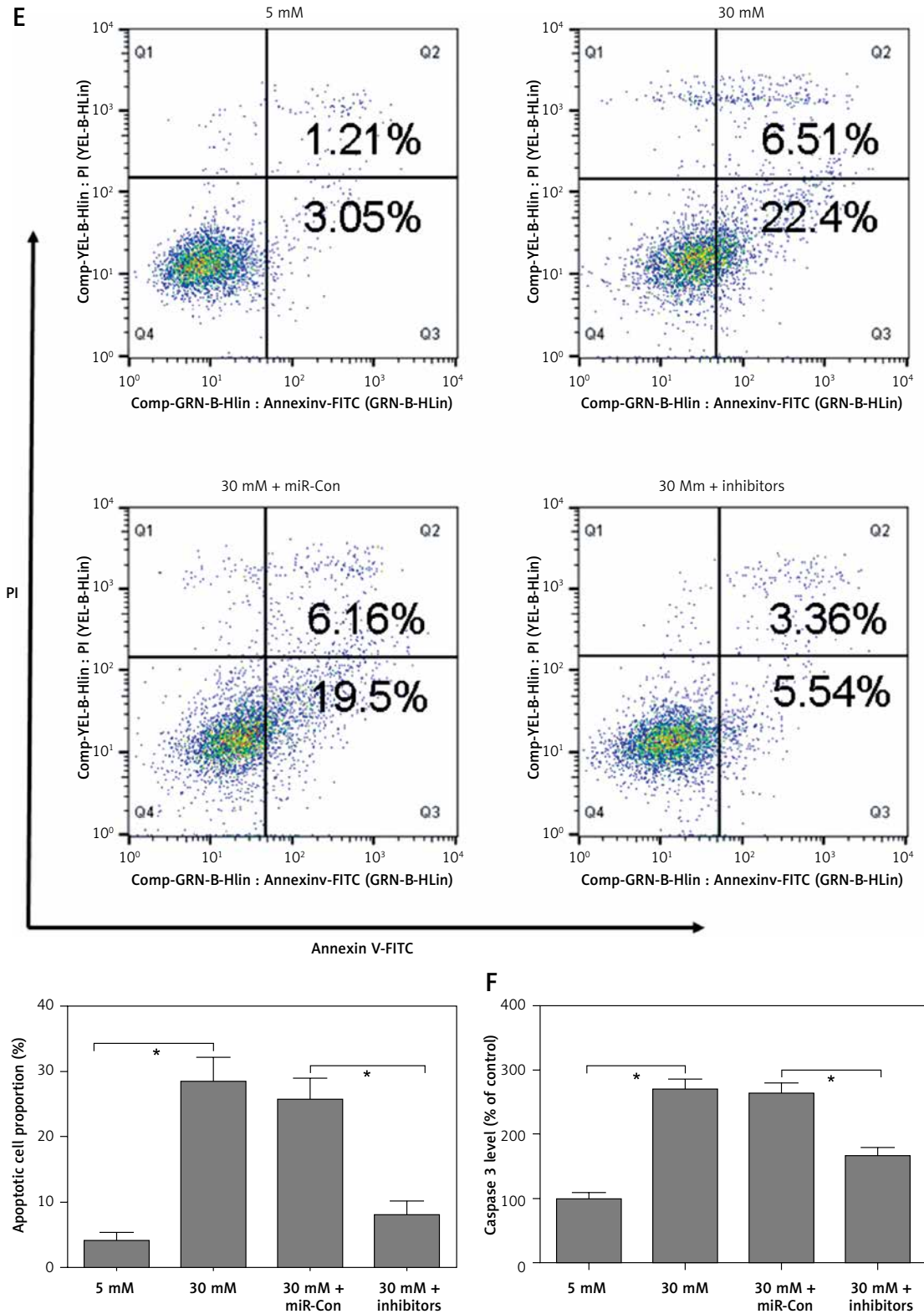


Figure 2. Cont. Annexinv-FITC double staining (E) and caspase3 level (F) in supernatant were used to assess cell apoptosis

* $P < 0.05$ means 30 mM + inhibitors group vs. 30 mM + miR-Con group. ** $P < 0.001$ means high glucose group (30 mM) vs. normal glucose group (5 mM).

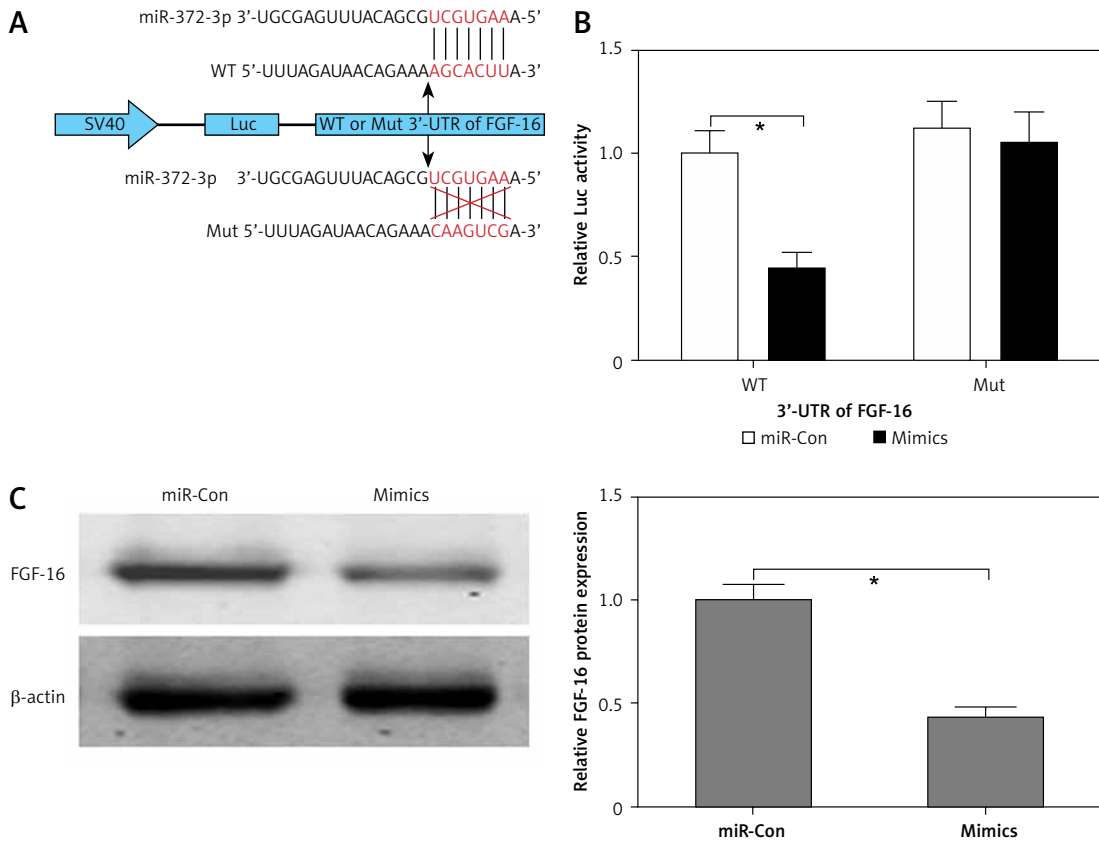


Figure 3. FGF-16 was a direct target of miR-372-3p. **A** – A conserved complementary pairing sequence between the 3'-UTR of FGF-16 and miR-372-3p was predicted using bioinformatics algorithm. **B** – Luciferase reporter gene assay. **C** – After transfection with miR-372-3p mimics or miR-Con into glomerular endothelial cells, FGF-16 protein expression was measured using western blotting

**P* < 0.05.

dothelial cell damage, we measured the effect of high glucose or miR-372-3p inhibitors on FGF-16 protein expression. High glucose stimulation significantly decreased the protein expression of FGF-16 in glomerular endothelial cells, while knockdown of miR-372-3p abolished the high glucose-induced inhibition of FGF-16 protein expression (Figures 4 A, B). We also found that transfection with FGF-16 overexpressed vectors into glomerular endothelial cells rescued the high glucose-induced reduction of FGF-16 protein expression (Figures 4 A, B). Transfection with FGF-16 overexpressed vectors or miR-372-3p inhibitors into high glucose-exposed glomerular endothelial cells possessed an equal effectiveness to improve FGF-16 protein expression (Figures 4 A, B). In addition, high glucose-triggered reduction of NO production (Figure 4 C), an increase in MDA (Figure 4 D), caspase 3 level (Figure 4 E) and apoptotic cell proportion (Figure 4 F) were abrogated by transfection with overexpressed FGF-16 plasmids into glomerular endothelial cells. These findings showed that overexpression of FGF-16 might protect against high glucose-induced glomerular endothelial cell dysfunction.

miR-372-3p is a potential diagnostic factor for DN

Compared with HC, the expression levels of miR-372-3p and miR-15a in plasma were significantly increased in T1DM (Figures 5 A, B) and T2DM (Figures 5 C, D) patients with DN. To explore whether miR-372-3p and miR-15a could serve as the diagnostic markers for DN, ROC with AUC was used to evaluate the diagnostic significance of miR-372-3p and miR-15a in DN. The ROC curve showed that the AUC of miR-372-3p and miR-15a was 0.805 (95% CI: 0.771–0.893) and 0.722 (95% CI: 0.625–0.819) for DN diagnosis in patients with T1DM, respectively (Table II, Figure 6 A). The sensitivity and specificity of miR-372-3p and miR-15a for DN diagnosis in patients with T1DM were 0.660 and 0.947, and 0.679 and 0.719, respectively (Table II and Figure 6 A). These results suggested that the diagnostic significance of miR-372-3p might be superior to miR-15a for DN diagnosis in patients with T1DM. In addition, ROC analysis was performed in the combination of miR-372-3p and miR-15a for DN diagnosis in patients with T1DM. The AUC of miR-372-3p combined with miR-15a

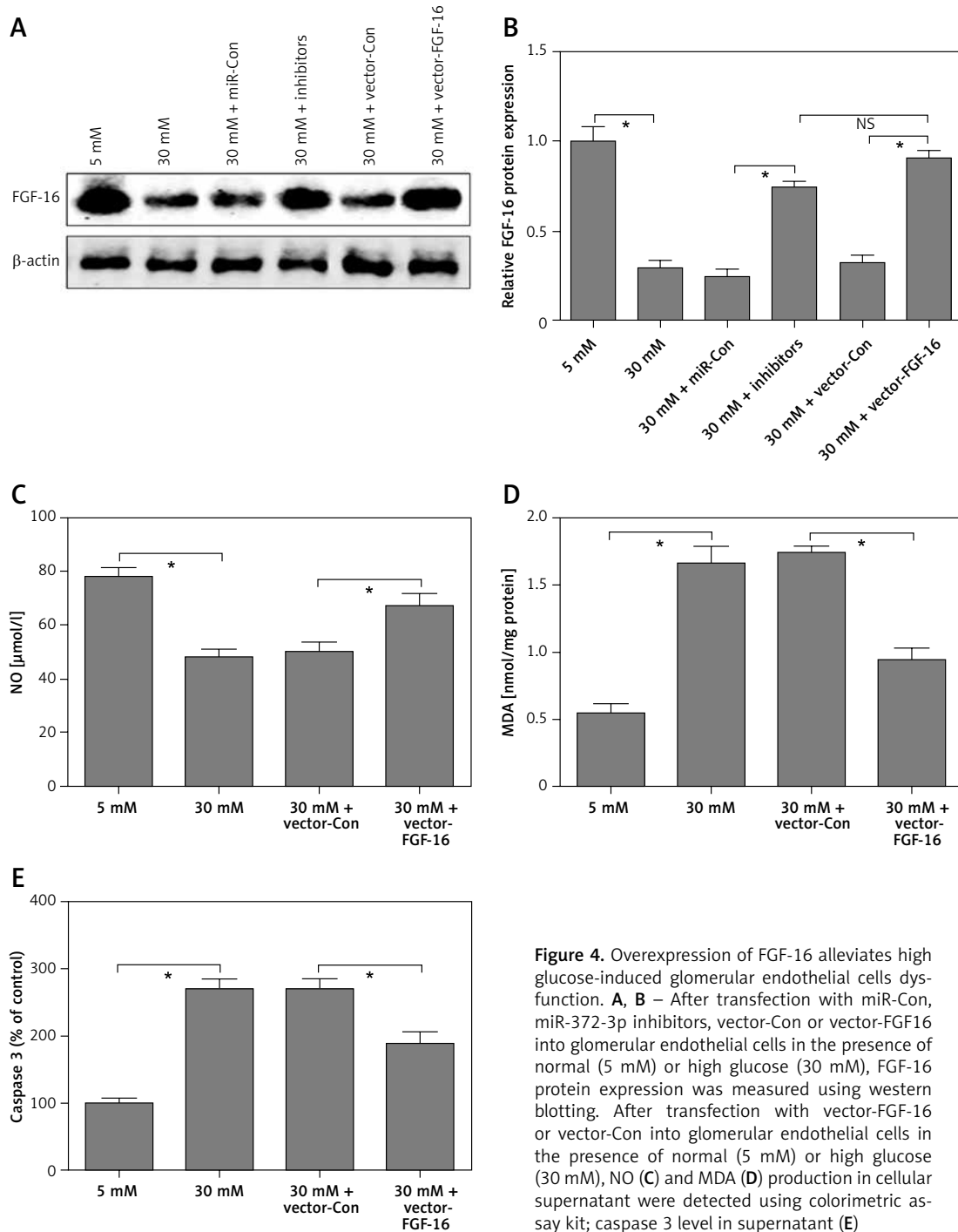


Figure 4. Overexpression of FGF-16 alleviates high glucose-induced glomerular endothelial cells dysfunction. **A, B** – After transfection with miR-Con, miR-372-3p inhibitors, vector-Con or vector-FGF16 into glomerular endothelial cells in the presence of normal (5 mM) or high glucose (30 mM), FGF-16 protein expression was measured using western blotting. After transfection with vector-FGF-16 or vector-Con into glomerular endothelial cells in the presence of normal (5 mM) or high glucose (30 mM), NO (**C**) and MDA (**D**) production in cellular supernatant were detected using colorimetric assay kit; caspase 3 level in supernatant (**E**)

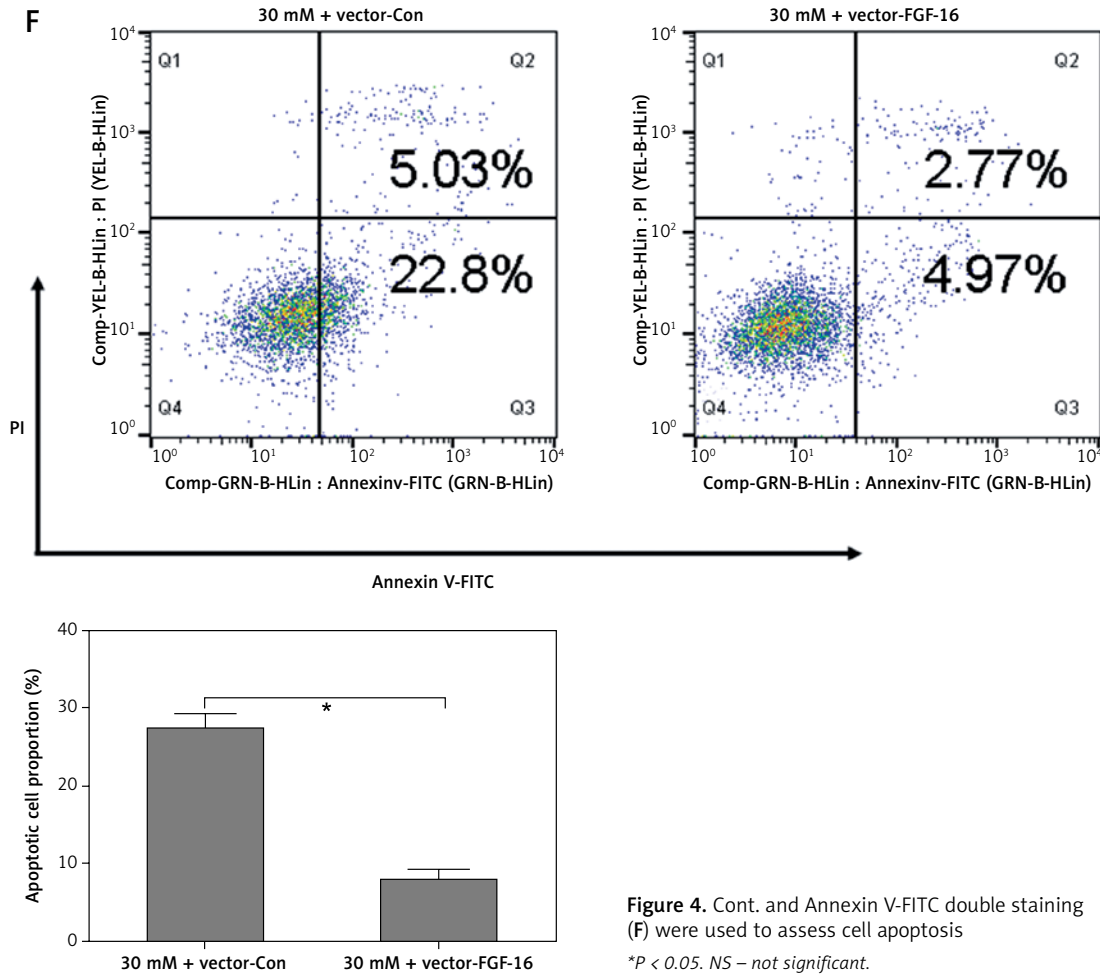
was 0.865 (95% CI: 0.793–0.936), with sensitivity of 0.679 and specificity of 0.947 (Table II, Figure 6 A). These findings suggested that the diagnostic significance of the miR-372-3p combined with miR-15a might be better than miR-372-3p or miR-15a for DN diagnosis alone.

We also found that miR-372-3p combined with miR-15a for DN diagnosis in patients with T2DM showed a good sensitivity (0.831) and specificity (0.912) with a high AUC value (0.922 with 95% CI: 0.883–0.961). These results also indicated that the diagnostic significance of miR-372-3p might

be superior to miR-15a for DN diagnosis in patients with T2DM, while miR-372-3p combined with miR-15a possessed a higher clinical value in the diagnosis of DN in patients with T2DM (Table II and Figure 6 B).

Discussion

In our study, we carried out a miR microarray for exploring the underlying molecular mechanisms of high glucose-induced glomerular endothelial cell damage. Our results demonstrated that



miR-372-3p expression level was elevated in high glucose-stimulated glomerular endothelial cells and might be closely related to high glucose-induced glomerular endothelial cell dysfunction, reflecting that it induced cell growth inhibition and apoptosis, inhibited eNOS/NO system activity and promoted MDA production. Also, we observed that FGF-16 as a direct target of miR-372-3p could be post-transcriptionally repressed by miR-372-3p and performed cytoprotection in high glucose-induced glomerular endothelial cell injuries. We also revealed that miR-372-3p and miR-15a were sensitive and specific markers for the diagnosis of DN patients with T1DM or T2DM. More importantly, combination of miR-372-3p and miR-15a showed a higher positive diagnostic rate for distinguishing T1DM or T2DM patients with DN from healthy subjects. These results corroborated the view that miR-372-3p might possess important pathogenetic and diagnostic implications for DN.

Recently, miRs have been authenticated as key mediators in the pathogenesis of DN, suggesting that circulating miRs may serve as potential markers for evaluating DN progression [9]. Circulating and urinary miRs are identified as promising non-invasive biomarkers for DN diagnosis, which con-

tributes to the stability and detectability of miRs in body fluids and exosomes [27]. Several studies have revealed that serum, plasma and urinary miRs, including urinary exosome-derived miRs, can be developed as biomarkers for DN screening [13–15, 28, 29]. For instance, plasma miR-21-5p, miR-29a-3p and miR-126-3p are deregulated in the progression of DN [30, 31]. Murray *et al.* highlight that serum miR-372-3p is significantly elevated in pediatric patients with extracranial malignant germ-cell tumors (GCTs) compared with healthy volunteers, and miR-372-3p (AUC = 1.00; $p = 0.001$) enables sensitive diagnosis of pediatric extracranial malignant GCTs [32, 33]. miR-15a has been identified as a potential diagnostic biomarker for stroke (specificity = 98.7%) [34]. Wang *et al.* document miR-15a as a biomarker to distinguish sepsis from systemic inflammatory response syndrome in human subjects (AUC = 0.858, 95% CI: 0.800–0.916, sensitivity = 68.3%, specificity = 94.4%) [35]. In the present study, miR-372-3p and miR-15a were significantly up-regulated in the plasma of T1DM and T2DM patients with DN compared with HC. ROC analysis revealed that the diagnostic value of miR-372-3p, miR-15a or miR-372-3p combined with miR-15a in T2DM patients

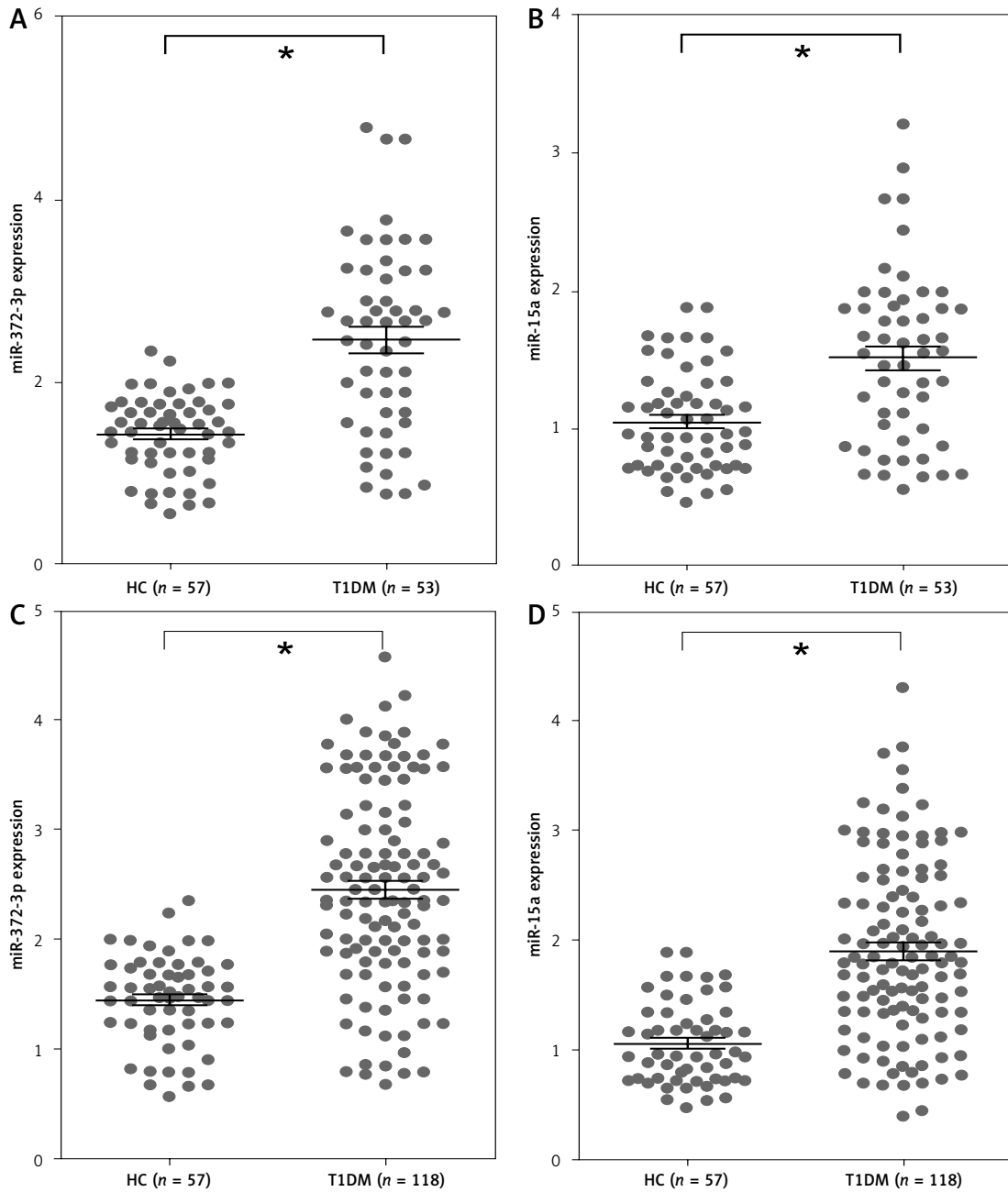


Figure 5. miR-372-3p and miR-15a were up-regulated in plasma of T1DM or T2DM patients. miR-372-3p and miR-15a expression levels in plasma were measured using RT-qPCR in T1DM (A, B) and T2DM (C, D) patients

* $P < 0.05$.

Table II. Performance of miR-372-3p and miR-15a in the differential diagnosis of DN from HC

Parameter	AUC	P-value	95% CI		Sensitivity	Specificity	Youden index	Cutoff point
			Lower	Upper				
T1DM with DN:								
miR-372-3p	0.805	< 0.001	0.771	0.893	0.660	0.947	0.607	1.985
miR-15a	0.722	< 0.001	0.625	0.819	0.679	0.719	0.398	1.204
miR-15a + miR-372-3p	0.865	< 0.001	0.793	0.936	0.679	0.947	0.626	3.618
T2DM with DN:								
miR-372-3p	0.841	< 0.001	0.783	0.898	0.763	0.860	0.623	1.825
miR-15a	0.822	< 0.001	0.762	0.882	0.737	0.807	0.544	1.342
miR-15a + miR-372-3p	0.922	< 0.001	0.883	0.961	0.831	0.912	0.743	3.008

HC – healthy controls, DN – diabetic nephropathy, T1DM – type 1 diabetes mellitus, T2DM – type 2 diabetes mellitus, AUC – area under the receiver operating characteristic curve, CI – confidence interval.

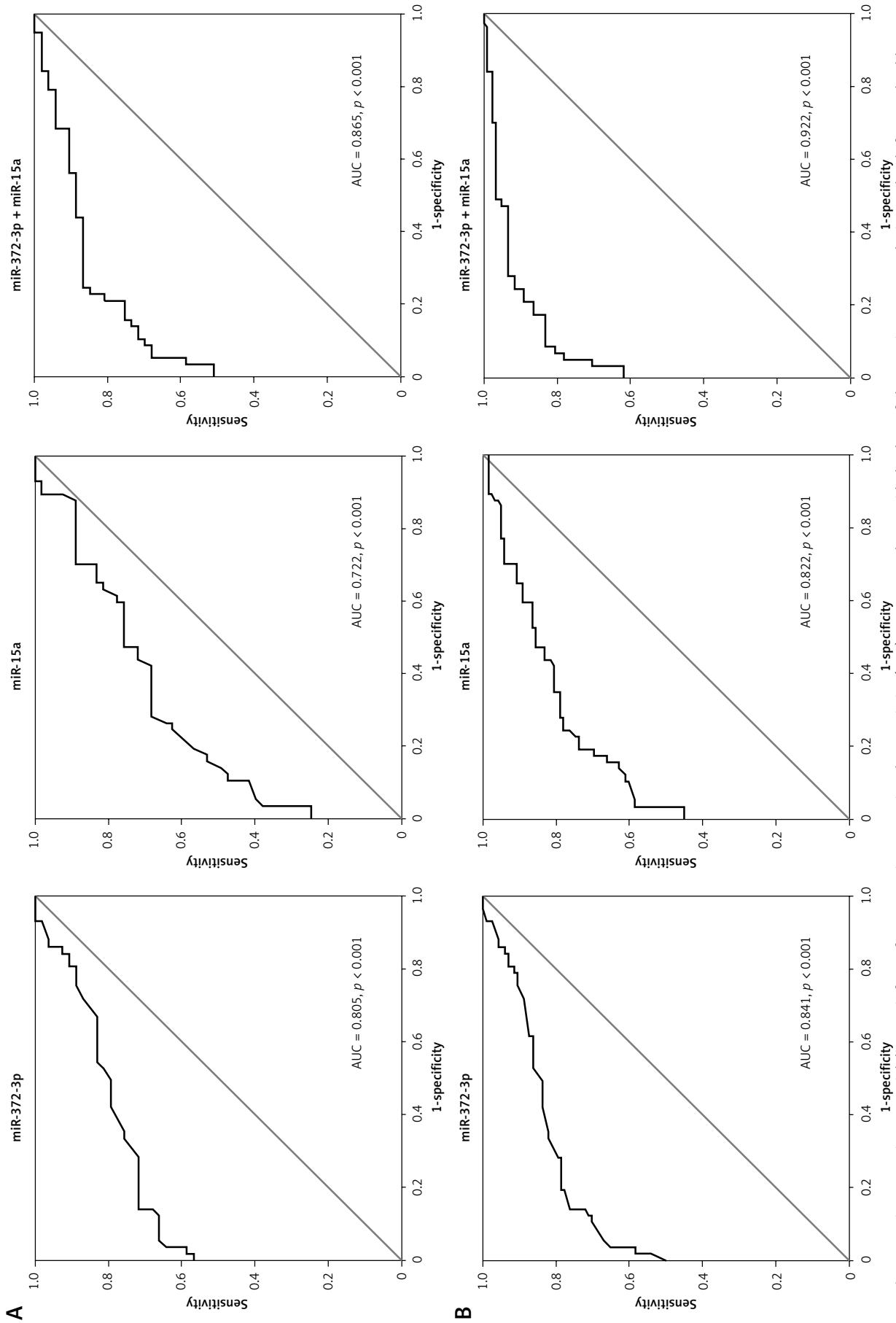


Figure 6. miR-372-3p is a potential diagnostic factor for DN. Receiver operating characteristics (ROC) curves were drawn with the data of plasma miR-372-3p and miR-15a levels from 57 healthy controls and 53 patients with T1DM (A), as well as 57 healthy controls and 118 patients with T2DM (B). Using binary logistic regression analysis, the ROC curves were drawn with the data of plasma miR-372-3p combined with miR-15a for DN diagnosis

(AUC = 0.841, $p < 0.001$; AUC = 0.822, $p < 0.001$ or AUC = 0.922, $p < 0.001$) with DN was better than that in T1DN patients (AUC = 0.805, $p < 0.001$; AUC = 0.722, $p < 0.001$ or AUC = 0.865, $p < 0.001$) with DN.

miR-372-3p has been reported as a serum biomarker for cancer diagnosis and as an oncogene promoting cancer cell proliferation and invasion [36, 37]. However, its precise function in high glucose-induced glomerular endothelial cell dysfunction remains unclear. In our study, the increased miR-372-3p expression in glomerular endothelial cells might be due to the high glucose stimulation. Experimental measurements demonstrated that knockdown of miR-372-3p in glomerular endothelial cells impeded the development of high glucose-induced endothelial disorders. Importantly, a target gene, FGF-16, of miR-372-3p was associated with high glucose-induced glomerular endothelial cell dysfunction. In agreement with cytoprotection of miR-372-3p loss-of-function in glomerular endothelial cells, overexpressed FGF-16 showed the ability to attenuate high glucose-induced cell injuries. These results suggested that miR-372-3p/FGF-16 might play a key role in maintaining endothelial homeostasis.

FGF-16 is predominantly expressed in the heart and plays a crucial role in postnatal cardiac development [38]. FGF-16 has been described as being inhibited in the pathological processes of cardiotoxicity [39]. Moreover, FGF-16 as a growth factor exhibits significant mitogenic activity for primary embryonic brown adipocytes [40]. FGF-16 has also been reported to promote endothelial cell migration, while it fails to induce endothelial cell proliferation [41]. We observed that exposure of glomerular endothelial cells in high glucose resulted in a decrease in FGF-16 protein expression, suggesting that downregulation of FGF-16 might predispose to high glucose-induced glomerular endothelial cell injuries due to its protective effects in endothelial homeostasis.

In conclusion, our results suggest that miR-372-3p might be considered as a potential glucose responsive miRNA participating in high glucose-induced glomerular endothelial cell dysfunction and as a potential diagnostic biomarker for DN screening.

Conflict of interest

The authors declare no conflict of interest.

References

1. Mohamed Q, Gillies MC, Wong TY. Management of diabetic retinopathy: a systematic review. *JAMA* 2007; 298: 902-916.
2. Finne P, Reunanen A, Stenman S, Groop PH, Gronhagen-Riska C. Incidence of end-stage renal disease in patients with type 1 diabetes. *JAMA* 2005; 294: 1782-7.
3. Remuzzi G, Macia M, Ruggenenti P. Prevention and treatment of diabetic renal disease in type 2 diabetes: the BENEDICT study. *J Am Soc Nephrol* 2006; 17: S90-97.
4. Kanwar YS, Wada J, Sun L, et al. Diabetic nephropathy: mechanisms of renal disease progression. *Exp Biol Med* 2008; 233: 4-11.
5. Cheng H, Harris RC. Renal endothelial dysfunction in diabetic nephropathy. *Cardiovasc Hematol Disord Drug Targets* 2014; 14: 22-33.
6. Denli AM, Tops BB, Plasterk RH, Ketting RF, Hannon GJ. Processing of primary microRNAs by the microprocessor complex. *Nature* 2004; 432: 231-5.
7. Beltrami C, Simpson K, Jesky M, et al. Association of elevated urinary miR-126, miR-155, and miR-29b with diabetic kidney disease. *Am J Pathol* 2018; 188: 1982-92.
8. Huang Y, Liu Y, Li L, et al. Involvement of inflammation-related miR-155 and miR-146a in diabetic nephropathy: implications for glomerular endothelial injury. *BMC Nephrol* 2014; 15: 142.
9. Assmann TS, Recamonde-Mendoza M, de Souza BM, Bauer AC, Crispim D. MicroRNAs and diabetic kidney disease: systematic review and bioinformatic analysis. *Mol Cell Endocrinol* 2018; 477: 90-102.
10. Liu F, Zhang S, Xu R, Gao S, Yin J. Melatonin attenuates endothelial-to-mesenchymal transition of glomerular endothelial cells via regulating miR-497/ROCK in diabetic nephropathy. *Kidney Blood Press Res* 2018; 43: 1425-36.
11. Lv C, Zhou YH, Wu C, Shao Y, Lu CL, Wang QY. The changes in miR-130b levels in human serum and the correlation with the severity of diabetic nephropathy. *Diabetes Metab Res Rev* 2015; 31: 717-24.
12. Jia Y, Guan M, Zheng Z, et al. miRNAs in urine extracellular vesicles as predictors of early-stage diabetic nephropathy. *J Diabetes Res* 2016; 2016: 7932765.
13. Li W, Yang S, Qiao R, Zhang J. Potential value of urinary exosome-derived let-7c-5p in the diagnosis and progression of type ii diabetic nephropathy. *Clin Lab* 2018; 64: 709-18.
14. Wang J, Duan L, Tian L, et al. Serum miR-21 may be a potential diagnostic biomarker for diabetic nephropathy. *Exp Clin Endocrinol Diabetes* 2016; 124: 417-23.
15. Assmann TS, Recamonde-Mendoza M, Costa AR, et al. Circulating miRNAs in diabetic kidney disease: case-control study and in silico analyses. *Acta Diabetol* 2019; 56: 55-65.
16. Yu W, Huang X, Tian X, et al. GATA4 regulates Fgf16 to promote heart repair after injury. *Development* 2016; 143: 936-49.
17. Pippitt K, Li M, Gurgle HE. Diabetes mellitus: screening and diagnosis. *Am Fam Physician* 2016; 93: 103-9.
18. Zhou X, Wen W, Shan X, et al. A six-microRNA panel in plasma was identified as a potential biomarker for lung adenocarcinoma diagnosis. *Oncotarget* 2017; 8: 6513-25.
19. Sun Y, Mei H, Xu C, Tang H, Wei W. Circulating microRNA-339-5p and -21 in plasma as an early detection predictors of lung adenocarcinoma. *Pathol Res Pract* 2018; 214: 119-25.
20. Tong YS, Wang XW, Zhou XL, et al. Identification of the long non-coding RNA POU3F3 in plasma as a novel biomarker for diagnosis of esophageal squamous cell carcinoma. *Mol Cancer* 2015; 14: 3.
21. Yu FY, Xie CQ, Sun JT, Peng W, Huang XW. Overexpressed miR-145 inhibits osteoclastogenesis in RANKL-induced bone marrow-derived macrophages and ovarioctomized mice by regulation of Smad3. *Life Sci* 2018; 202: 11-20.

22. Wang L, Wei Y, Yan Y, et al. CircDOCK1 suppresses cell apoptosis via inhibition of miR196a5p by targeting BIRC3 in OSCC. *Oncol Rep* 2018; 39: 951-66.
23. Cheng H, Wang H, Fan X, Pauksakon P, Harris RC. Improvement of endothelial nitric oxide synthase activity retards the progression of diabetic nephropathy in db/db mice. *Kidney Int* 2012; 82: 1176-83.
24. Luo Z, Fujio Y, Kureishi Y, et al. Acute modulation of endothelial Akt/PKB activity alters nitric oxide-dependent vasomotor activity in vivo. *J Clin Invest* 2000; 106: 493-9.
25. Komers R, Schutzer WE, Reed JF, et al. Altered endothelial nitric oxide synthase targeting and conformation and caveolin-1 expression in the diabetic kidney. *Diabetes* 2006; 55: 1651-9.
26. Wang HW, Jiang X, Zhang Y, et al. FGF21 protects against hypoxia injury through inducing HSP72 in cerebral microvascular endothelial cells. *Front Pharmacol* 2019; 10: 101.
27. Assmann TS, Recamonde-Mendoza M, De Souza BM, Crispim D. MicroRNA expression profiles and type 1 diabetes mellitus: systematic review and bioinformatic analysis. *Endocr Connect* 2017; 6: 773-90.
28. Motawi TK, Shehata NI, ElNokeety MM, El-Emady YF. Potential serum biomarkers for early detection of diabetic nephropathy. *Diabetes Res Clin Pract* 2018; 136: 150-8.
29. Argyropoulos C, Wang K, Bernardo J, et al. Urinary microRNA profiling predicts the development of microalbuminuria in patients with type 1 diabetes. *J Clin Med* 2015; 4: 1498-517.
30. Bijkerk R, Duijs JM, Khairoun M, et al. Circulating microRNAs associate with diabetic nephropathy and systemic microvascular damage and normalize after simultaneous pancreas-kidney transplantation. *Am J Transplant* 2015; 15: 1081-90.
31. Pezzolesi MG, Satake E, McDonnell KP, Major M, Smiles AM, Krolewski AS. Circulating TGF-beta1-regulated miRNAs and the risk of rapid progression to ESRD in type 1 diabetes. *Diabetes* 2015; 64: 3285-93.
32. Murray MJ, Bell E, Raby KL, et al. A pipeline to quantify serum and cerebrospinal fluid microRNAs for diagnosis and detection of relapse in paediatric malignant germ-cell tumours. *Br J Cancer* 2016; 114: 151-62.
33. Murray MJ, Huddart RA, Coleman N. The present and future of serum diagnostic tests for testicular germ cell tumours. *Nat Rev Urol* 2016; 13: 715-25.
34. Lu WJ, Zeng LL, Wang Y, et al. Blood microRNA-15a correlates with IL-6, IGF-1 and acute cerebral ischemia. *Curr Neurovasc Res* 2018; 15: 63-71.
35. Wang H, Zhang P, Chen W, Feng D, Jia Y, Xie LX. Evidence for serum miR-15a and miR-16 levels as biomarkers that distinguish sepsis from systemic inflammatory response syndrome in human subjects. *Clin Chem Lab Med* 2012; 50: 1423-8.
36. Wang Q, Liu S, Zhao X, Wang Y, Tian D, Jiang W. MiR-372-3p promotes cell growth and metastasis by targeting FGF9 in lung squamous cell carcinoma. *Cancer Med* 2017; 6: 1323-30.
37. Syring I, Bartels J, Holdenrieder S, Kristiansen G, Muller SC, Ellinger J. Circulating serum miRNA (miR-367-3p, miR-371a-3p, miR-372-3p and miR-373-3p) as biomarkers in patients with testicular germ cell cancer. *J Urol* 2015; 193: 331-7.
38. Lu SY, Sontag DP, Detillieux KA, Cattini PA. FGF-16 is released from neonatal cardiac myocytes and alters growth-related signaling: a possible role in postnatal development. *Am J Physiol Cell Physiol* 2008; 294: C1242-9.
39. Wang J, Xiang B, Dolinsky VW, Kardami E, Cattini PA. Cardiac Fgf-16 expression supports cardiomyocyte survival and increases resistance to doxorubicin cytotoxicity. *DNA Cell Biol* 2018; 37: 866-77.
40. Konishi M, Mikami T, Yamasaki M, Miyake A, Itoh N. Fibroblast growth factor-16 is a growth factor for embryonic brown adipocytes. *J Biol Chem* 2000; 275: 12119-22.
41. Antoine M, Wirz W, Tag CG, et al. Fibroblast growth factor 16 and 18 are expressed in human cardiovascular tissues and induce on endothelial cells migration but not proliferation. *Biochem Biophys Res Commun* 2006; 346: 224-33.